

# Spectral densities of superconducting qubits with environmental resonances.

Kaushik Mitra, C. J. Lobb, and C. A. R. Sá de Melo  
*Joint Quantum Institute and Department of Physics*  
*University of Maryland College Park MD 20742*  
 (Dated: February 10, 2022)

PACS numbers: 74.50.+r, 85.25.Dq, 03.67.Lx

In this paper we derive the environmental spectral density for flux [1], phase [2] and charge [3] qubits when each of them is coupled to an environment with a resonance. From the spectral density we obtain the characteristic spontaneous emission (relaxation) lifetimes  $T_1$  for each of these qubits, and show that there is a substantial enhancement of  $T_1$  beyond the resonant frequency of the environment. The circuits considered are shown in Fig. 1, 2 and 3.

The flux qubit shown in Fig. 1 is measured by a dc-SQUID. Hence to study decoherence and relaxation time scales, one has to consider the noise that is transferred from the qubit to the dc-SQUID.

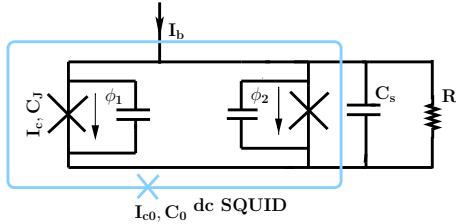


FIG. 1: Flux qubit measured by a dc-SQUID (gray line). The qubit is in the inner SQUID loop with critical current  $I_c$  and capacitance  $C_J$  for both junctions. The inner SQUID is shunted by a capacitance  $C_s$ , and environmental resistance  $R$  and is biased by a ramping current  $I_b$ . The dc-SQUID loop has junction capacitance  $C_0$  and critical current  $I_{c0}$ .

The classical equation of motion for the dc-SQUID is

$$C_0 \ddot{\phi} + \frac{2\pi}{\Phi_0} I_{c0} \sin \phi - \frac{2\pi}{\Phi_0} I + \int_0^t dt' Y(t-t') \dot{\phi}(t') = 0 \quad (1)$$

where  $\phi$  is the gauge invariant phase across the Josephson junction of the outer dc-SQUID loop,  $I_{c0}$  is the critical current of its junction,  $\Phi_0 = h/2e$  is the flux quantum, and the total induced current in the outer dc-SQUID is

$$I = \frac{4}{L_{dc}} \langle \delta\phi_0 \sigma_z \rangle + \frac{4}{L_{dc}} \langle \phi_m \rangle + \left( \frac{2\pi}{\Phi_0} \right)^2 J_1 \langle \phi_p \rangle. \quad (2)$$

Here  $\phi_p$  and  $\phi_m$  are the sum and difference of the gauge invariant phases across the junctions of the inner SQUID,  $L_{dc}$  is the self-inductance of the inner SQUID, and  $J_1$  is the bilinear coupling between  $\phi_m$  and  $\phi_p$  at the potential energy minimum. The term  $\delta\phi_0 = \pi M_q I_{cir} / \Phi_0$ , where  $I_{cir}$  is the circulating current of the localized states of the

qubit (described in terms of Pauli matrix  $\sigma_z$ ), and  $M_q$  is the mutual inductance between the qubit and the outer dc-SQUID. The last term in Eq. (1) is the dissipation term due to effective admittance  $Y(\omega)$  felt by the outer dc-SQUID.

For the charge qubit shown in Fig. 2 the classical equation of motion for the charge  $Q$  is

$$V_g(\omega) = \left( -\frac{\omega^2 L_J(\omega)}{1 - \omega^2 L_J(\omega) C_J} + \frac{1}{C_g} + i\omega Z(\omega) \right) Q(\omega) \quad (3)$$

Here,  $V_g$  is the gate voltage,  $C_g$  is the gate capacitance,  $L_J$  and  $C_J$  are the Josephson inductance and capacitance respectively,  $Z(\omega)$  is the effective impedance seen by the charge qubit due to a transmission line resonator (cavity),  $\Omega$  is the resonant frequency of the resonator, and  $Q$  is the charge across  $C_g$ .

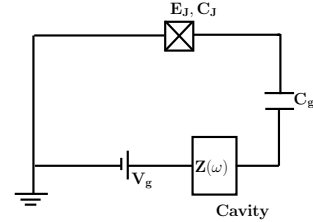


FIG. 2: Circuit diagram of the Cooper-pair box. The superconducting island is connected to a large reservoir through a Josephson junction with Josephson energy  $E_J$  and capacitance  $C_J$ . The voltage bias  $V_g$  is provided through a resonator (cavity) having environmental impedance  $Z(\omega)$ , which is connected to  $C_g$  as shown.

For the phase qubit shown in Fig. 3 the classical equation of motion is

$$C_0 \ddot{\gamma} + \frac{2\pi}{\Phi_0} I_{c0} \sin \gamma - \frac{2\pi}{\Phi_0} I + \int_0^t dt' Y(t-t') \dot{\gamma}(t') = 0 \quad (4)$$

where  $I_{c0}$  is the critical current of Josephson junction  $J$  in Fig.1,  $I$  is the bias current, and  $\Phi_0 = h/2e$  is the flux quantum. The last term is the dissipation term due to  $Y(\omega)$  which is the effective admittance as seen by the dc-SQUID.

The equations of motion described in Eqs. (1), (3), and (4), can be all approximately described by the effective spin-boson Hamiltonian

$$\tilde{H} = \frac{\hbar\omega_{01}}{2} \sigma_z + \sum_k \hbar\omega_k b_k^\dagger b_k + H_{SB}, \quad (5)$$

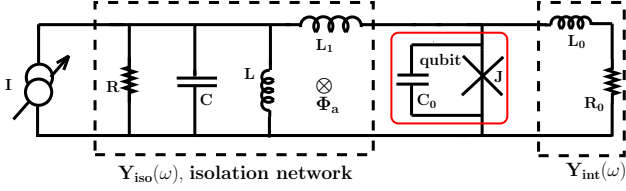


FIG. 3: Schematic drawing of the phase qubit with an RLC isolation circuit.

written in terms of Pauli matrices  $\sigma_i$  (with  $i = x, y, z$ ) and boson operators  $b_k$  and  $b_k^\dagger$ . The first term in Eq. (5) represents a two-level approximation for the qubit (system) described by states  $|0\rangle$  and  $|1\rangle$  with energy difference  $\hbar\omega_{01}$ . The second term corresponds to the isolation network (bath) represented by a bath of bosons, where  $b_k$  and  $b_k^\dagger$  are the annihilation and creation operator of the  $k$ -th bath mode with frequency  $\omega_k$ . The third term is the system-bath (SB) Hamiltonian which corresponds to the coupling between the environment and the qubit.

At the charge degeneracy point for the charge qubit (gate charge  $N_g = 0$ ), at the flux degeneracy point (external flux  $\Phi_{\text{ext}} = \pi\Phi_0$ ) for the flux qubit, and the suitable flux bias condition for the phase qubit (external flux  $\Phi_a = L_1\phi_0$ )  $H_{SB}$  reduces to,

$$H_{SB} = \frac{1}{2}\sigma_x\hbar\langle 1|v|0\rangle \sum_k \lambda_{k1} (b_k^\dagger + b_k) \quad (6)$$

where  $v = \phi$  for the flux qubit,  $Q$  for the charge qubit, and  $\gamma$  for the phase qubit. The spectral density of the bath modes  $J(\omega) = \hbar \sum_k \lambda_k^2 \delta(\omega - \omega_k)$  has dimensions of energy and can be written as  $J(\omega) = \omega \text{Re}Y(\omega)(\Phi_0/2\pi)^2$  for flux and phase qubits and  $J(\omega) = 2\hbar\omega e^2/\hbar \text{Re}Z(\omega)$  for charge qubits.

For the flux qubit circuit shown in Fig. 1, the shunt capacitance  $C_s$  is used to control the environment, while the Ohmic resistance of the circuit is modelled by  $R$ . In this case, the environmental spectral density is

$$J_1(\omega) = \frac{\alpha_1\omega}{(1 - \omega^2/\Omega_1^2)^2 + 4\omega^2\Gamma_1^2/\Omega_1^4}. \quad (7)$$

when  $\omega_m \gg \max(\omega_p, \omega_0)$ , and when the dc-SQUID is far away from the switching point to be modelled by an ideal inductance  $L_J$ . Here,  $\Omega_1 = 1/\sqrt{L_J C_s} = \sqrt{4\pi I_c/(C_s \Phi_0)}$  is the plasma frequency of the inner SQUID and plays the role of the resonant frequency, where  $I_c$  is the critical current for each of two Josephson junctions. Also,  $\Gamma_1 = 1/(C_s R)$  plays the role of the resonance width, and  $\alpha_1 = 2(eI_p I_b M_q)^2/(C_s^2 \hbar^2 R \Omega_1^4)$  reflects the low frequency behavior. The coupling between the flux qubit and the outer dc-SQUID occurs emerges from the interaction of the persistent current  $I_p$  of the qubit and the bias current  $I_b$  of the dc-SQUID via their mutual inductance  $M_q$ .

The spectral density for the charge qubit shown in Fig. 2 is obtained by solving for the normal modes of the resonator and transmission lines, including an input impedance  $R$  at each end of the resonator. It is given by

$$J_2(\omega) = \frac{e^2\Omega_2}{\ell c} \frac{\Gamma_2}{(\omega - \Omega_2)^2 + (\Gamma_2/2)^2} \quad (8)$$

where  $\Omega_2$  is the resonator frequency,  $\ell$  is resonator length,  $c$  is the capacitance per unit length of the transmission line,  $C_g$  is the gate capacitance, and  $C_J$  is the junction capacitance. The quantity  $\Gamma_2 = \Omega_2/Q$  where  $Q$  is the quality factor of the cavity.

For negligible  $Y_{\text{int}}(\omega)$ , the spectral density of the phase qubit shown in Fig. (3) is

$$J_3(\omega) = \left(\frac{\Phi_0}{2\pi}\right)^2 \frac{\alpha_3\omega}{(1 - \omega^2/\Omega_3^2)^2 + 4\omega^2\Gamma_3^2/\Omega_3^4}, \quad (9)$$

where  $\alpha_3 = L^2/((L + L_1)^2 R) \approx (L/L_1)^2/R$  is the leading order term in the low frequency ohmic regime,  $\Omega_3 = \sqrt{(L + L_1)/(LL_1 C)} \approx 1/\sqrt{LC}$  is essentially the resonance frequency, and  $\Gamma_3 = 1/(2CR)$  plays the role of resonance width. Here, we used  $L_1 \gg L$  corresponding to the relevant experimental regime.

Once the spectral functions of the environments are known, the relaxation rates are derived following standard methods [4]. At finite temperatures, the relaxation time

$$\frac{\hbar}{T_{1,i}} = \beta_i J_i(\omega) \coth \frac{\hbar\omega}{2k_B T} \quad (10)$$

is directly related to the environmental spectral density. Here, the index  $i = 1, 2, 3$  labels the results for flux, charge and phase qubits, respectively. The parameter  $\beta_i$  takes values  $\beta_1 = 1$  for the flux qubit of Fig. 1,  $\beta_2 = C_g^2/(C_g + C_J)^2$  for the charge qubit of Fig. 2 and  $\beta_3 = 1/[(\Phi_0/2\pi)^2 C_0 \omega_{01}]$  for the phase qubit of Fig. 3. An inspection of Eq. (10) and the corresponding spectral functions  $J_i(\omega)$  shows that suitably detuning the qubit to higher frequencies beyond the environmental resonance can enhance the characteristic spontaneous emission lifetime (relaxation time)  $T_{1,i}$  of the qubit by a couple of orders of magnitude as discussed in Ref. [5].

- 
- [1] J. E. Mooij *et al*, Science **285**, 1036 (1999)
  - [2] J. Martinis *et al.*, Phys. Rev. Lett. **89**, 117901 (2002)
  - [3] A. Wallraff *et al*, Nature **431** 162 (2004)
  - [4] U. Weiss, *Quantum Dissipative Systems*, World Scientific (1999).
  - [5] K. Mitra, C. J. Lobb, and C. A. R. Sá de Melo, e-print arXiv:0712.1064 (2007).